

Model Predictive Direct Current Control

Juan C. Ramirez Martinez.
Electrical Machines
and Drives Laboratory
Wuppertal University
42219 Wuppertal, Germany
Tel: +49 (202) 439 1867
Fax: +49 (202) 439 1824
jcmartinez@ieee.org

Ralph M. Kennel
Department of Electrical Drives
and Power Electronics
Technical University of Munich
80333 Munich, Germany
Tel: +49 089 289-28358
Fax: +49 089 289-28336
Email: kennel@ieee.org

Tobias Geyer
Department of Electrical and
Computer Engineering
The University of Auckland
1052 New Zealand
Tel: +64 (9) 373 7599 ext 89634
Fax: +64 (9) 373 7461
t.geyer@ieee.org

Abstract—This paper presents a model predictive current controller and its application to ac electrical drives. In a stationary reference frame, the proposed control scheme keeps both the alpha and beta current within given hysteresis bounds while minimizing the switching frequency of the inverter. Based on an internal model of the drive, the controller predicts the drive's future behavior for each switching sequence, extrapolates the output trajectories and selects the inverter switch positions (voltage vector) that minimizes the switching frequency and keeps the predicted current trajectories within the hysteresis bounds. This scheme carries several important advantages. As all computations are performed on-line, all quantities may be time varying including model parameters, set-points and hysteresis bounds. Besides that, the scheme is applicable to a large class of (three-phase) ac electrical machines driven by inverters and it is also effective under all operating conditions, including transients and zero stator frequency operation. Specially, the very fast transient response of hysteresis control scheme is inherited.

I. INTRODUCTION

Current control of a three-phase drive is one of the most important subjects in power electronics and has been widely studied in the last decades. Linear methods like proportional integral controllers using pulsewidth modulation (PWM) and nonlinear methods like hysteresis control are well documented in the literature [1], [2] and [3].

Nowadays, with the development of faster and more powerful microprocessors, the implementation of new and more complex schemes is possible. One of these complex schemes, Model Predictive Control (MPC) was developed at the end of the seventies in the petrochemical industry [4]. Using an internal mathematical model of the plant, the plant's future behavior is predicted over a prediction horizon for the admissible set of control variables. The control objectives are given in a cost function. By minimizing the latter subject to the plant model and constraints, the optimal values for the control variables are determined. This is a very powerful concept that generalized the predictive control schemes used so far in the power electronics community. A classification of MPC is available in [5].

Variants of predictive control have been applied in power converters with different purpose [6], for example in drives [7], active filters [8] and power factor correction [9].

Naturally, predictive control has been also applied in current control for inverters [10] and [11]. In this approaches predictive control is used to calculate the necessary load voltage to optimize the current behavior. Here, a modulator is used to generate this desired voltage. In this approach, the converter is simply modelled as a gain. A modification of these methods calculate the duty cycle of the PWM pulses necessary for the current control [12].

One advantage of predictive control is the possibility to include nonlinearities of the drive in the mathematical model and hence the behavior of the variables for different switching states can be calculated directly. This property was exploited in earlier studies. In [13] the predictive control is used to minimize the switching frequency of the voltage source inverter (VSI). Also in [14] and [15] this property is used to minimize the current error for each switching state of the VSI.

A conceptually approach based on MPC and applied to the Direct Torque Control problem is presented in [16], [17] and [18].

This paper presents the afore mentioned method introduced in [17] and [18]. Here it is applied to control the current of a three-phase drive while minimizing the switching frequency. The currents in the $\alpha\beta$ coordinate system are to be kept within given hysteresis bounds. This on-line optimization scheme is derived by adopting the principles of constrained optimal control with a receding horizon policy. Over a short switching horizon all switching sequences are considered. Based on the measured currents, for each switching sequence, the evolution of the state variable is predicted by an internal model of the drive. It is determined which switching sequences yield current trajectories that are either feasible at the end of the switching horizon or, if the current are outside of the bounds, reduce the violation of the bounds at all time-steps within the switching horizon. These sequences are referred to as candidate sequences.

To emulate a long output horizon, the current trajectories of candidate sequences are extrapolated, and the number of time-steps is determined for which these quantities are kept within their hysteresis bounds. For each switching sequence, an approximation of the average switching frequency is computed. It is given by the total number of switch transitions

in the sequence divided by the time duration of the extrapolated trajectory. Minimizing the switching frequency over all switching sequences, the cost function in this case, yields the optimal sequence of switch transitions. Of this sequence, only the first element is applied to the drive, thus establishing a receding horizon policy.

The paper is structured as follows. Section II summarizes the physical model of the drive, while Section III reformulates this model so that it can be used as prediction model in. The model predictive current controller is detailed in Section IV. In this paper, the controller is available only in one form with a switching horizon of $N = 1$. Simulation results for two ways of having the control input are drawn in Section V. Finally, Section VI draws conclusions about the proposed control scheme, while the appendix shows the matrices of the prediction model.

II. PHYSICAL MODEL

Throughout the document, we will use the normalized time $\tau = \omega_{sR} \cdot t$, where ω_{sR} is the rated value of the stator frequency. Additionally we will use $\xi(\tau)$, $\tau \in \mathbb{R}$ to denote continuous-time variable and $\xi(k)$, $k \in \mathbb{N}$ to denote discrete-time variables with the corresponding sampling interval T_s .

All variables $\xi_{abc} = [\xi_a \ \xi_b \ \xi_c]^T$ in the three-phase system (abc) are transformed to $\xi_{\alpha\beta 0} = [\xi_\alpha \ \xi_\beta \ \xi_0]^T$ in the orthogonal $\alpha\beta 0$ stator reference frame through:

$$\xi_{\alpha\beta 0} = P \xi_{abc} \quad (1)$$

where P is the matrix of the well-known Park transformation.

A. Physical Model of the Inverter

The representation of a two-level IGBT voltage source inverter driving an induction motor is shown in Fig. 1

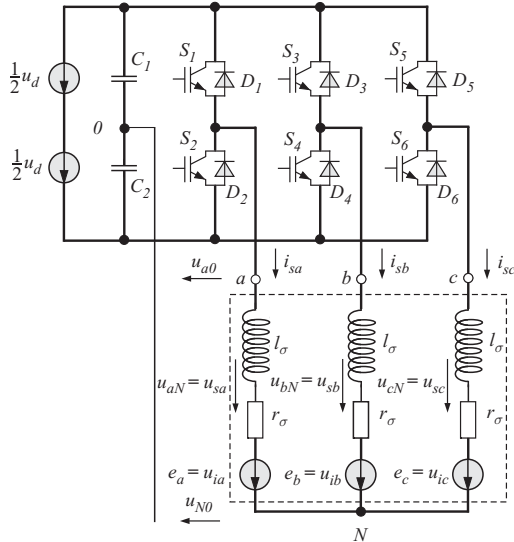


Fig. 1: Voltage Source Inverter driving an induction motor.

The inverter consists of three half-bridge units; the upper and lower power switches of each unit are alternating turned on and off, at given time instants. Each of the three output

terminals can be connected to either the positive dc-link voltage potential $+\frac{u_d}{2}$, or to the negative potential $-\frac{u_d}{2}$, depending on the state of the switches in the respective half-bridge. Such switching states of the inverter are determined by the gating signals S_a , S_b and S_c as follows

$$S_a = \begin{cases} 1, & \text{if } S_1 \text{ on and } S_2 \text{ off} \\ 0, & \text{if } S_1 \text{ on and } S_2 \text{ on} \end{cases} \quad (2)$$

$$S_b = \begin{cases} 1, & \text{if } S_3 \text{ on and } S_4 \text{ off} \\ 0, & \text{if } S_3 \text{ on and } S_4 \text{ on} \end{cases} \quad (3)$$

$$S_c = \begin{cases} 1, & \text{if } S_5 \text{ on and } S_6 \text{ off} \\ 0, & \text{if } S_5 \text{ on and } S_6 \text{ on} \end{cases} \quad (4)$$

and can be expressed in vectorial form as:

$$\mathbf{S} = \frac{2}{3} (S_a + \mathbf{a}S_b + \mathbf{a}^2S_c) \quad (5)$$

where $\mathbf{a} = e^{j\frac{2\pi}{3}}$.

A total of $N_u = 2^3 = 8$ different arrangements are therefore possible. They are selected by the firing signals at the gates of the power semiconductors. The output voltages represented by space vector are defined as:

$$\mathbf{u}_k = \frac{2}{3} (u_{aN} + \mathbf{a}u_{bN} + \mathbf{a}^2u_{cN}) \quad (6)$$

Then, the output voltage can be represented in terms of the switching state vector \mathbf{S} by:

$$\mathbf{u}_k = u_d \cdot \mathbf{S} \quad (7)$$

where u_d is the DC link voltage.

B. Physical Model of the Induction Motor

The load system fed by the VSI could be any RL-EMF circuit, as it is shown in [14]. In this case, the purpose is to feed a squirrel-cage induction motor. Here, the output voltage \mathbf{u}_k of the inverter is equal to the stator voltage \mathbf{u}_s of the induction motor. The representation of the motor [19] is based on the equivalent circuit that can be seen inside of the dashed box in Fig. 1. The stator voltage from the machine is calculated as:

$$\mathbf{u}_s = r_\sigma \cdot \mathbf{i}_s + l_\sigma \cdot \frac{d\mathbf{i}_s}{d\tau} + \mathbf{u}_i \quad (8)$$

Here, the equivalent resistance r_σ is expressed by $r_\sigma = r_s + k_r^2 r_r$ and $l_\sigma = \sigma l_s$ is the leakage inductance of the machine, where $\sigma = 1 - \frac{l_m^2}{l_s l_r}$ is the total leakage factor and $k_r = \frac{l_m}{l_r}$ is the coupling factor of the rotor. The term \mathbf{u}_i represents the cross coupling from the rotor to the stator winding through the induced voltage. The value of \mathbf{u}_i can be calculated directly from (8). However, our purpose is to apply this current control in a field Oriented control scheme, where the rotor flux ψ_r is already known. Then \mathbf{u}_i is calculated by:

$$\mathbf{u}_i = -\frac{k_r}{\tau_r} (j\omega\tau_r - 1) \cdot \psi_r \quad (9)$$

Since our purpose is to manipulate the input voltage in order to control the current, and besides the dynamics must be modelled in a stator $\alpha\beta 0$ reference frame, then Eq. (8) and (9)

must be re-written. Here the stator current $i_{s\alpha}$ and $i_{s\beta}$; and the rotor flux linkages $\psi_{r\alpha}$ and $\psi_{r\beta}$ are used as state variables. The input voltages $u_{s\alpha}$ and $u_{s\beta}$ are the stator voltages also in stator reference frame. The model parameters are the angular velocity ω of the rotor shaft, the main inductance l_m , the transient stator time constant $\tau_\sigma' = \frac{\sigma l_s}{r_\sigma}$, the rotor time constant $\tau_r = \frac{l_r}{r_r}$, the mechanical time constant of the machine τ_m and the variable load torque T_L . The state equations are:

$$i_{s\alpha} + \tau_\sigma' \frac{di_{s\alpha}}{d\tau} = \frac{k_r}{r_\sigma \tau_r} \psi_{r\alpha} + \frac{k_r}{r_\sigma} \omega \psi_{r\beta} + \frac{1}{r_\sigma} u_{s\alpha} \quad (10)$$

$$i_{s\beta} + \tau_\sigma' \frac{di_{s\beta}}{d\tau} = \frac{k_r}{r_\sigma \tau_r} \psi_{r\beta} - \frac{k_r}{r_\sigma} \omega \psi_{r\alpha} + \frac{1}{r_\sigma} u_{s\beta} \quad (11)$$

$$\psi_{r\alpha} + \tau_r \frac{d\psi_{r\alpha}}{d\tau} = -\omega \tau_r \psi_{r\beta} + l_m i_{s\alpha} \quad (12)$$

$$\psi_{r\beta} + \tau_r \frac{d\psi_{r\beta}}{d\tau} = \omega \tau_r \psi_{r\alpha} + l_m i_{s\beta} \quad (13)$$

$$\tau_m \cdot \frac{d\omega}{d\tau} = T_e - T_L \quad (14)$$

Equations (10)-(14) represent the standard dynamic model of an induction motor, where the saturation of the machine's magnetic field, the changes of the rotor resistance due to skin effect, and the temperature changes of the stator resistance are neglected.

III. INTERNAL MODEL OF THE CONTROLLER

In this section, we derive a discrete-model of the drive that is suitable to serve as an internal prediction model for the predictive controller proposed in the next section. The purpose of this model is to predict the trajectory of both stator currents.

As the time-constant of the rotor speed dynamics exceeds the length of the prediction interval by several orders of magnitude, the rotor speed dynamic is neglected and the speed is assumed to remain constant within the prediction horizon. This allows us to treat the speed as a model parameter rather than a state, thus removing equation (14) from the rotor model.

We define the overall state vector of the drive as:

$$\mathbf{x} = [i_{s\alpha} \quad i_{s\beta} \quad \psi_{r\alpha} \quad \psi_{r\beta}]^T \quad (15)$$

the gating signals S_a , S_b and S_c as the input vector

$$\mathbf{u} = [S_a \quad S_b \quad S_c]^T \in \{1, 0\} \quad (16)$$

and both stator current signals as output vector

$$\mathbf{y} = [i_{s\alpha} \quad i_{s\beta}]^T \quad (17)$$

Combining the motor model (10)-(14) and using forward Euler approximation approach, the following discrete-time model of the drive is derived.

$$\mathbf{x}(k+1) = (I + \mathbf{A}T_s) \cdot \mathbf{x}'(k) + T_s \cdot \mathbf{B}\mathbf{u}(k) \quad (18)$$

$$\mathbf{y}(k) = \mathbf{C}\mathbf{x}(k) \quad (19)$$

In this model, I denotes the identity matrix and T_s is the sampling interval. The definition of the matrices \mathbf{A} and \mathbf{B} can be found in the appendix.

IV. PROPOSED MODEL PREDICTIVE CURRENT CONTROL STRATEGY

As described in [16] and [17], and adopting the principles of MPC, we present a control methodology that considers all (admissible) switching sequences over a rather short switching horizon N , which is referred to as the control horizon in the MPC community. A switching sequence is defined as a sequence of semiconductor switch positions \mathcal{S} , over the time-interval of length N from time step 0 to time-step $N - 1$. In a next step, based on the nonlinear discrete-time prediction model (18) and (19), the MPC scheme computes for each switching sequences the drive's response, i.e. the evolution of the output variables over the switching horizon N . To emulate a long output horizon, the "promising" output trajectories are extrapolated, and the number of time-steps is determined when the first output variable hits a hysteresis bound. The cost associated with each switching sequence is determined by dividing the total number of switch transitions in the sequence by the length of the extrapolated trajectory. Minimizing this penalty yields the optimal switching sequence and the next optimal switch position to be applied to the inverter.

The model predictive scheme can be developed in two forms, with $N > 1$ and $N = 1$, differing mostly in the degree of freedom for the switching sequences thus in the computational burden and the performance.

A. Horizon $N=1$

The computational burden imposed by the model predictive scheme with a switching horizon $N > 1$ might exceed the capabilities of some existing control hardware. To reduce the computation time while dealing with the issue of infeasibility, we use a scheme that uses a switching horizon $N = 1$.

Given the current state $x(k)$, the last switch position $u(k - 1)$, the bounds on the output variables and using the nonlinear discrete-time prediction model of the drive, the controller computes at the time-instant k the next switch position $u(k)$ according to the following procedure:

- 1) Given the last control input $u(k - 1)$, 8 possible control inputs result.
- 2) For these sequences, compute the system response, i.e. compute all open-loop α, β current trajectories starting from $x(k)$ over the horizon N .
- 3) Determine those input sequences, which have output trajectories that are *feasible* at the end of, or *pointing in the proper direction* for all time-steps within the horizon. We refer to these switching sequences as *candidate* sequences $U^i(k)$ with $i \in \mathcal{I}_c \subseteq \mathcal{I}$. Feasibility means that the output variable lies within corresponding bounds at time-step $k + N$; to point in the proper direction refers to the case in which an output variable is not necessary feasible, but the degree of the bound's violation decreases at every time-step within the switching horizon. The above conditions need to hold *componentwise*, i.e. for output variables.
- 4) • If there are candidate switching sequences ($\mathcal{I}_c \neq \{\}$): Extrapolate the output trajectories from

time-instant $k + 1$ on linearly using the samples at k and $k + 1$. Derive the numbers of time-steps when the first of the two output variables leaves the feasible region defined by the corresponding upper and lower bound. This yields the number of time-steps before the next predicted switching n_i , $i \in \mathcal{I}_c$.

- If there are no candidate input vectors ($\mathcal{I}_c = \{\}$): Consider all voltage vectors by setting $\mathcal{I}_c = \{1, 2, \dots, 8\}$ and compute for each voltage vector u^i , $i \in \mathcal{I}_c$, the worst case violation of the bounds on any of the output variables

$$\eta_i = \max\{\eta_{i_\alpha}^i, \eta_{i_\beta}^i\} \quad (20)$$

- 5) • If there are candidate input vectors, compute for each input vector candidate u_i the cost:

$$c_i = \frac{\|u_i(k) - u(k-1)\|_2}{n_i} \quad (21)$$

where $\|u_i(k+1) - u_i(k)\|_2$ is the total number of switch transitions necessary to apply the input vector $u_i(k+1)$ given the last applied input $u(k)$.

- If there are no candidate input vectors, consider again all voltage vectors setting $\mathcal{I}_c = \{1, 2, \dots, 8\}$ and assign to each one the cost:

$$c_i = \eta_i \quad (22)$$

- 6) Choose the input sequence $U^i(k)$ with the minimum cost, where i is given by:

$$i = \arg \min_{i \in \mathcal{I}_c} c_i \quad (23)$$

- 7) Apply the switch position $u_k = U^i(k)$ and shift the horizon by one time-step.

At the next time-instant the above procedure would be repeated, however, the average computation time could be reduced to be kept at a minimum. This can be achieved by first evaluating whether switching can be avoided altogether. It means, when computing the next switch position, whether the output variables are at time-step $k+N$ within their respective bounds when reapplying the last switch position for N time-steps, then the actual switch position will be reapplied. Only if this simple test fails, the above outlined computations need to be performed again.

Example 1: To visualize the control concept, consider the example shown in Fig. 2. Assume there are three switching sequences $U^i(k)$, $i \in \mathcal{I}_c = \{1, 2, 3\}$ over the switching horizon $N = 2$. According to the definition, $U^1(k)$ and $U^2(k)$ are candidate sequences, whereas $U^3(k)$ is not. Extrapolating the α and β currents trajectories and determining when they leave the feasible region leads to the results summarized in Table I.

Minimizing the cost yields the sequence $U^2(k)$ as the optimum. Note that this solution requires two switch transitions (one at time-instant k , the second one at time-instant $k+1$), but this investment pays out due to the longer length

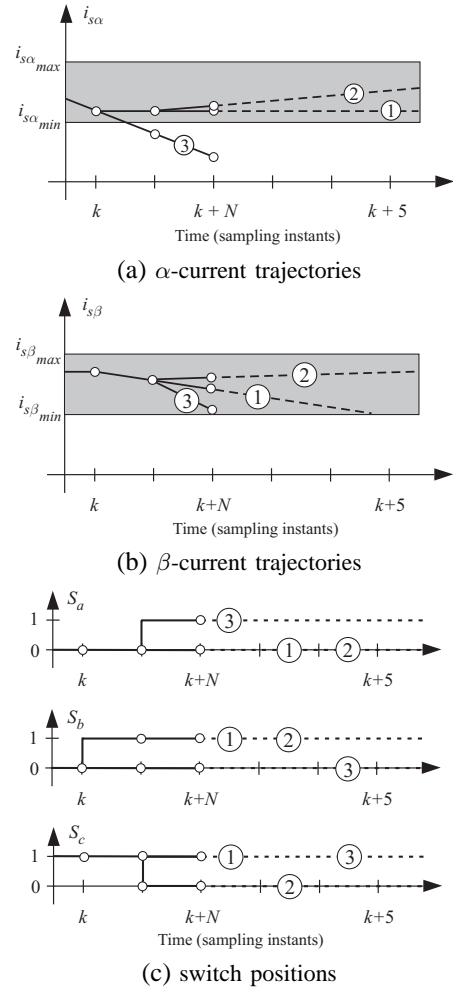


Fig. 2: α - β trajectories of Example 1.

Sequence number i	Total length n_i of the (extrapolated) sequence	Number of switch transitions s_i	Cost c_i
1	4	1	1/4
2	10	2	2/10
3	-	-	-

TABLE I: Characteristics of the switching sequences in Example 1

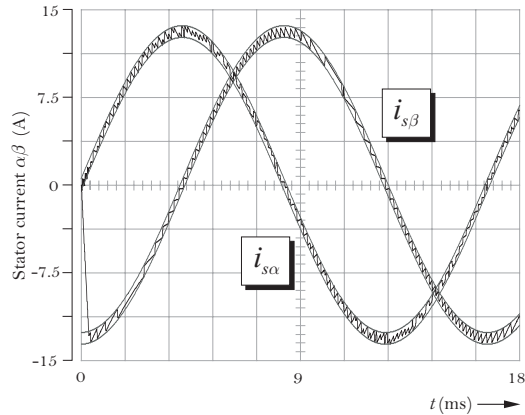
of the output trajectory. Without extrapolation, the controller would select $U^1(k)$ as the optimum, since the corresponding cost expressions would be $\frac{1}{2}$ and $\frac{2}{2}$ for $U^1(k)$ and $U^2(k)$, respectively. In the long run, however, this choice would be inferior compared with $U^2(k)$ thus motivating the concept of extrapolation.

V. SIMULATION RESULTS

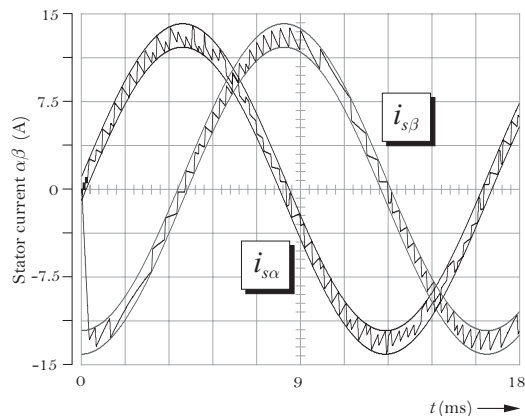
Simulations of the proposed predictive control scheme have been carried out with Matlab-Simulink, in order to evaluate its performance. The results have been obtained with a sampling time of $T_s = 20.48 \mu s$. Every test was developed with a sinusoidal reference of 13.09A amplitude and 60Hz frequency. The drive employed for the analysis is constituted by a 4.5KW asynchronous machine and a 20kVA two-levels

IGBT inverter. The parameters of the machine are: stator resistance $r_s = 1.73\Omega$, rotor resistance $r_r = 0.8845\Omega$, stator and rotor leakage inductances $l_{s\sigma} = l_{r\sigma} = 3.67\text{mH}$ and mutual inductance $l_m = 82.19\text{mH}$

The first test was developed following the outlined computations described Section IV-A. Fig. 3(a) shows the developed currents α and β . when the bound width is set to 1.0A. Here it can be seen that both currents signal never violate their bounds.



(a) bound width of 1.0A



(b) bound width of 2.0A

Fig. 3: α - β current trajectories.

To demonstrate the performance of the scheme with a different bound width, it is modified from 1.0 A to 2.0 A. The Fig. 3(b) shows the obtained results. As it was expected, enlarging the bound width has the consequence of decreasing the switching frequency. The continuous line of Fig 4 shows how the switching frequency can be reduced, while enlarging the bound width.

To analyze the dynamic performance, the reference current $i_{s\alpha}^*$ is modified from 13.09A to 3.9A at instant $t = 16\text{ms}$, and the reference current $i_{s\beta}^*$ from 13.09A to 6.5A at instant $t = 17\text{ms}$. The dynamic performance is presented in Fig. 5.

Having a look at the Figs. 3(a) and 3(b), it could be thought that the proposed current predictive control has a similar performance than a classical hysteresis controller. In order to disperse possible misunderstandings, the performance of a

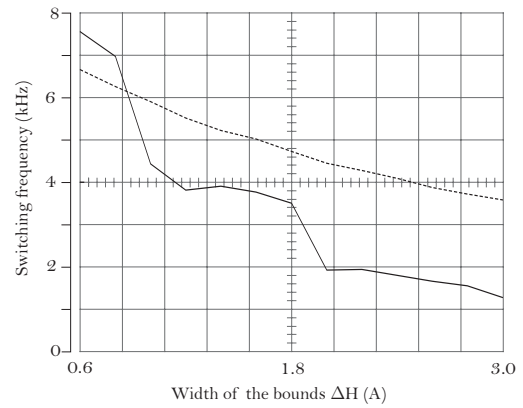


Fig. 4: Relationship between switching frequency and bound width.

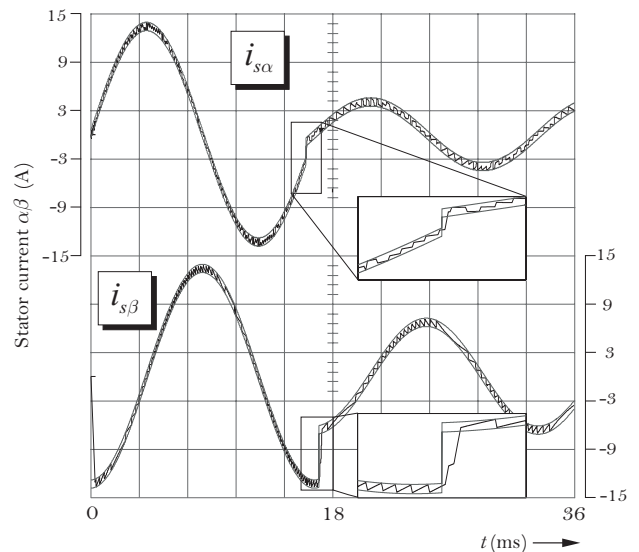


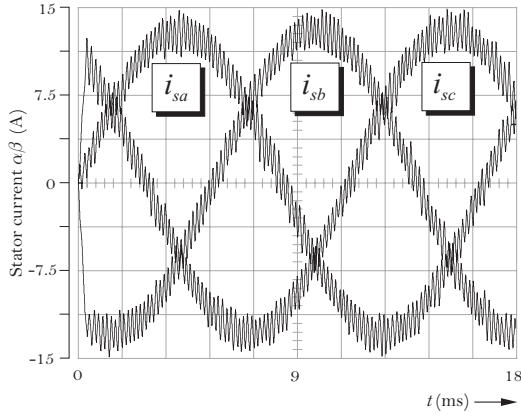
Fig. 5: Current trajectories with a bound width of 1.0A and reference changes

hysteresis controller was tested under similar conditions. The obtained abc stator currents are shown in Fig. 6(a). To have an easy comparison, the $\alpha\beta$ currents of Fig 3(a) were transformed into abc , shown in Fig 6(b). To figure out how the switching frequency reacts when enlarging the bound width, a similar test was done with the hysteresis control. The dotted line in Fig. 4 shows the results.

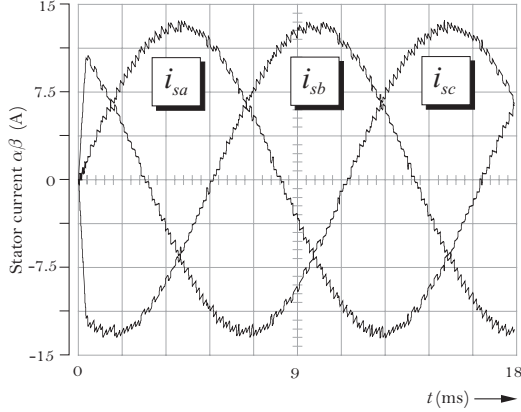
VI. CONCLUSION

In this paper, a model predictive drive controller with hysteresis bounds is applied to the current problem. It is based on an internal controller model, a controller objective function an optimization stage and an extrapolation step. The optimization process is performed over an one-step switching prediction horizon, which could be extended to multiple steps. The prediction horizon, however, is significantly longer than one step due to the extrapolation approach

As stated in [17], the proposed control scheme is highly flexible. It is straightforward to incorporate additional or different performance and control objectives by simply modifying



(a) Classical hysteresis controller



(b) Model predictive controller

Fig. 6: Three-phase stator currents, with a bound width of 1.0A

the cost function. Moreover, the controller can be directly applied to a large class of three-phase ac drives, only adapting the internal model. This adaption can be done on-line as a parameter adaption to account for a varying rotor resistance for example, or it can be done off-line, as a model structure change to make the controller applicable to another drive with different inverter topology and/or different electrical machine. Besides that, the only parameter to be tuned, is the bound width.

Although in a simple look, the proposed model predictive controller could be seen as kind of classical hysteresis control, here it is demonstrated that selecting the appropriate switching sequence based on the plant's behavior allows to have a controller that keeps the controlled output within their bound limits without incrementing the switching frequency.

VII. APPENDIX

The matrices of the model drive (18) and (19) are:

$$\mathbf{A} = \begin{bmatrix} -\frac{1}{\tau_{\sigma'}} & 0 & \frac{k_r}{r_{\sigma}\tau_r\tau_{\sigma'}} & \frac{k_r\omega}{r_{\sigma}\tau_{\sigma'}} \\ 0 & -\frac{1}{\tau_{\sigma'}} & -\frac{k_r\omega}{r_{\sigma}\tau_{\sigma'}} & \frac{k_r}{r_{\sigma}\tau_r\tau_{\sigma'}} \\ \frac{l_m}{\tau_r} & 0 & -\frac{1}{\tau_r} & -\omega \\ 0 & \frac{l_m}{\tau_r} & \omega & -\frac{1}{\tau_r} \end{bmatrix} \quad (24)$$

$$\mathbf{B} = \begin{bmatrix} \frac{2}{3r_{\sigma}\tau_{\sigma'}} & -\frac{1}{3r_{\sigma}\tau_{\sigma'}} & -\frac{1}{3r_{\sigma}\tau_{\sigma'}} \\ 0 & \frac{1}{\sqrt{3}r_{\sigma}\tau_{\sigma'}} & -\frac{1}{\sqrt{3}r_{\sigma}\tau_{\sigma'}} \\ 0 & 0 & 0 \\ 0 & 0 & 0 \end{bmatrix} \quad (25)$$

REFERENCES

- [1] J. Holtz, "Pulsewidth modulation electronic power conversion," in *Proc. IEEE*, Aug. 1994, pp. 1194–1214.
- [2] M. P. Kazmierkowski, R. Krishnan, and F. Blaabjerg, *Control in Power Electronics*. New York, USA: Academic, 2002.
- [3] N. Mohan, T. M. Undeland, and W. P. Robbins, *Power Electronics*. New York, USA: Wiley, 1995, 2nd ed.
- [4] E. Camacho and C. Bordons, *Model Predictive Control*. London, UK: Springer-Verlag, 1999.
- [5] A. Linder, "Modellbasierte praediktivregelung in der antriebstechnik," Ph.D. dissertation, Bergische Universitaet Wuppertal, Wuppertal, 2005, (in German).
- [6] S. Kuoro, P. Cortés, R. Vargas, U. Ammann, and J. Rodríguez, "Model predictive control - a simple and powerful method to control power converters," *IEEE Trans. Ind. Electron.*, vol. 56, no. 6, pp. 1826–1838, Jun. 2009.
- [7] R. Kennel and A. Linder, "Predictive control of inverter supplied electrical drives," in *Proc. IEEE Power Electronics Specialist Conference (PESC'00)*, Galway, Ireland, 2000, (CD-ROM).
- [8] P. Malesani, P. Mattavelli, and S. Buso, "Robust dead-beat current control for pwm rectifier and active filters," *IEEE Trans. Ind. Appl.*, vol. 35, no. 3, pp. 613–620, May/Jun. 1999.
- [9] P. Mattavelli, G. Spiazzi, and P. Tenti, "Predictive digital control of power factor pre-regulators," in *Proc. IEEE Power Electronics Specialist Conference (PESC'03)*, Acapulco, Mexico, 2003, (CD-ROM).
- [10] H. Le-Huy, K. Slimani, and P. Viarouge, "Analysis and implementation of a real-time predictive current controller for permanent-magnet synchronous servo drives," *IEEE Trans. Ind. Electron.*, vol. 41, no. 1, pp. 110–117, Feb. 1994.
- [11] O. Kukrer, "Discrete-time current control of voltage-fed three-phase pwm inverters," *IEEE Trans. Ind. Electron.*, vol. 11, no. 2, pp. 260–269, Mar. 1996.
- [12] W. Zhang, G. Feng, and Y. Liu, "Analysis and implementation of a new pfc digital control method," in *Proc. IEEE Power Electronics Specialist Conference (PESC'03)*, Acapulco, Mexico, 2003, pp. 335–340.
- [13] J. Holtz and S. Stadfeld, "A predictive controller for the stator current vector of ac-machines fed from a switched voltage source," in *Proc. IEEE International Power Electronics Conference (IPEC'83)*, vol. 2, Tokyo, Japan, 1983, pp. 1665–1675.
- [14] J. Rodríguez, J. Pontt, C. Silva, P. Correa, P. Lezana, P. Cortés, and U. Ammann, "Predictive current control of a voltage source inverter," *IEEE Trans. Ind. Electron.*, vol. 54, no. 1, pp. 495–503, Feb. 2007.
- [15] D. Schroeder, "Predictive control strategies for converter and inverter," in *Proc. IEEE International Conference on Industrial Technology (ICIT'09)*, 2009, pp. 1–8.
- [16] T. Geyer, "Low complexity model predictive control in power electronics and power systems," Ph.D. dissertation, Swiss Federal Institute of Technology, Zurich, 2005.
- [17] T. Geyer, G. Papafotiou, and M. Morari, "Model predictive direct torque control-part i: Concept, algorithm and analysis," *IEEE Trans. Ind. Appl.*, vol. 56, no. 6, pp. 1894–1905, Jun. 2009.
- [18] G. Papafotiou, J. Kley, K. Papadopolus, P. Bohren, and M. Morari, "Model predictive direct torque-part ii: Implementation and experimental evaluation," *IEEE Trans. Ind. Appl.*, vol. 56, no. 6, pp. 1906–1915, Jun. 2009.
- [19] J. Holtz, "The induction motor - a dynamic system," in *Proc. Annual Conference of the IEEE Industrial Electronics Society (IECON'94)*, vol. 1, Bologna, Italy, 1994, pp. P1–P6.